UNDERLIGNING THERMOCAPILLARY EFFECTS BY ELECTRON BEAM MELTING OF THIN SPECIMENS

L. Domergue[1], D. Camel[2] , S. Marya*

*Ecole Centrale de Nantes, BP 92101 44321 Nantes (F), Surendar.Marya@ec-nantes.fr
[1] Bourgogne Hydro,
[2] CEREM/DEM/SPCM, CEA Grenoble (France)

ABSTRACT

Extensive investigations on cast to cast variations observed in steels have underlined the role of thermo-capillary or surface tension driven fluid flow in welding operations. The behavior of weld pool under the electric arc is however affected by possible arc modifications linked to microchemistry variations in materials & this limits to some extent the real contribution from surface tension effects. Thus, electron beam welding with high vacuum was used to investigate thermo-capillary effects on thin austenitic stainless steels & nickel based alloys. The weld pool was monitored by video observations to estimate the importance of fluid flow during the melting & solidification phase. The results underline the importance of fluid flow on final solidification.

KEY WORDS
Surface tension, Stainless steels, Electron beam melting, Weld pool

1 Introduction

Surface tension is a measure of atomic cohesive forces and as such is expected to decrease with increasing temperatures. Thus normally pure metals and compounds have negative gradients of surface tension (γ) with temperature. However in presence of some surface active species, this normal evolution of surface tension with temperature can be reversed i.e., $d\gamma/dT$ can become positive . As very high temperatures and temperature gradients prevail over the pool during welding, important surface tension variations result in strong thermocapillary currents, which significantly influence the resulting weld profile. For example, deeper welds are generated with positive $d\gamma/dT$ which induce inward melt flow as schematically shown in Figure 1. It may be mentioned that very minor chemistry variations may completely change the sign of $d\gamma/dT$. In case of steels, it is generally thought that 50 to 80ppm of sulphur can be favourable for deeper welds subsequent to positive variation of surface temperature with temperature. Such minor variations in base metal chemistry are in compliance with usual material specifications and explain cast to cast variations often observed particularly in steels and nickel base alloys [1],[2],[3]. Further, surface tension that defines the wetting or spreading capacity of a liquid , is expected to affect the solidification cracking of welds [4]. In fact, not only the weld profile, but also the temperature gradients and solute partition at solid liquid interface during solidification are conditioned by the surface tension gradients in the weld pool. Higher gradients would imply stronger convection currents, propitious for solute mixing and probably finer grains through nucleation from broken segments of dendrites.

In the present work, we would present results on melting and solidification of thin specimens in a electron beam chamber with a view to simulate stationary weld pools. From fundamental point of view, this method of investigating surface tension effects in molten weld pools has some intrinsic advantages. For example, it is possible to minimize electromagnetic effect in the melt, contrary to arc welding where liquid movements and base metal chemistry affect the arc characteristics, which in turn affect weld pool dynamics. Further, vacuum melting is ideal for investigating minor chemistry effects due to absence of ambient contamination. The results presented here underline the importance of surface tension & thermocapillary flow in molten pool on solidification structures. It is suggested that even in materials with very low level of surface active species, due to solute partition during solidification, melt flow may undergo complete directional change during its solidification [5].
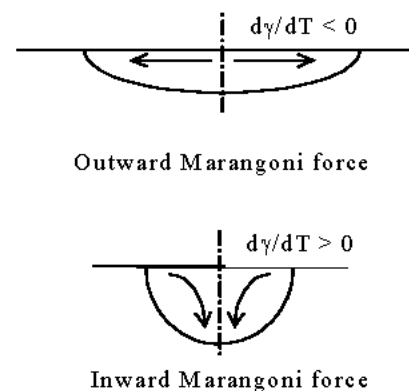
Fig.1 Factors affecting weld pool formation

2.Expérimental

Figure 2 shows the general experimental setup involving a electron beam unit which was constantly monitored for chamber conditions and process parameters. Specimens involved 20 and 14 mm diameter disks of 2 and 0,5 mm thickness. Electron beam is accelerated under 10KV, the emission current is monitored by filament current and overall heating power for specimen melting is completely controlled. Emission currents of 15mA to 60mA are used for 0,5 mm specimens implying 150 to 600 W of injected power. The electron beam spot over the specimen is kept fixed at $15\ 10^{-6}\ m^2$, which corresponds to specific powers of 10 à 40 GW/m². All specimens are properly cleaned according to a well defined procedure, so as maintain identical working conditions. Emission current is started at the initial pressure of 10^{-6} Pa which is composed essentially of hydrogen as the partial oxygen pressure is then as low as 10^{-8} Pa. These experimental conditions were thought important as oxygen is known to be a surface active element. The melt pool is filmed with a video camera fitted with infrared filters and in some cases melt flow velocity could be estimated through real time position of some floating particles. The temperature gradients in the pool could be controlled also through the cooling conditions of the clamping crucible.

3 Experimental Results

3. 1 Heating Period

The liquid motion in stationary thermal regime could be seen through some very small particles in the molten pool. In case of high sulfur steels (80ppm), the particles are found to converge towards the center of the molten pool, whereas in very pure materials, they are pushed outwards and remain confined to the periphery of the pool. This effect is related to the convection currents in the molten pool, which is outwards in pure metals and inwards in metals with surface active species, sulfur in the

Fig. 2 Experimental set up for electron beam melting, Circled 14 is the specimen holder with controlled cooling

present case. Further as seen in Figure 3, from the luminosity of the pool, the temperature distributions are different depending on the direction of the said convection currents. In low sulfur steels, a significant part of the melt surface seems to be at high temperatures and covers a major section of the molten pool, whereas in high sulfur steel specimens, only the central part of the melt pool seems to be at high temperatures. Thus it appears that under similar processing conditions, the surface temperatures in low sulfur steels are higher than those in high sulfur steels, as anticipated from liquid movements in the heating period. These direct observations of the molten pool, difficult in TIG welding due to the presence of the electric arc, confirmed the end results in two cases. For example, TIG welds were deeper in high sulfur steels, whereas low sulfur steels produced wider beads with shallow penetrations at identical process parameters[6]. The surface sections of the melted specimens, as shown in Table 1 and Figure 4 further confirmed the TIG welding results. Higher molten sections on the back surface of the specimens are seen in high sulfur steel, which strongly suggests that heat was preferentially conveyed to the inside of the pool. This thermal transfer would reduce the overall temperature of the front surface of the molten pool as observed earlier in Fig.3 right. In this case, only the central region of the pool is expected to be relatively hot. Thus, the qualitative temperature distributions and the molten profiles are all in line with the observed particle movements, which reflect the direction of convection currents in the pool. From the solidification ripples on the back surface (Fig.4), it is interesting to observe that high sulfur steels with larger molten sections are also prone to large weld fluctuations. Such instabilities were observed during the heating
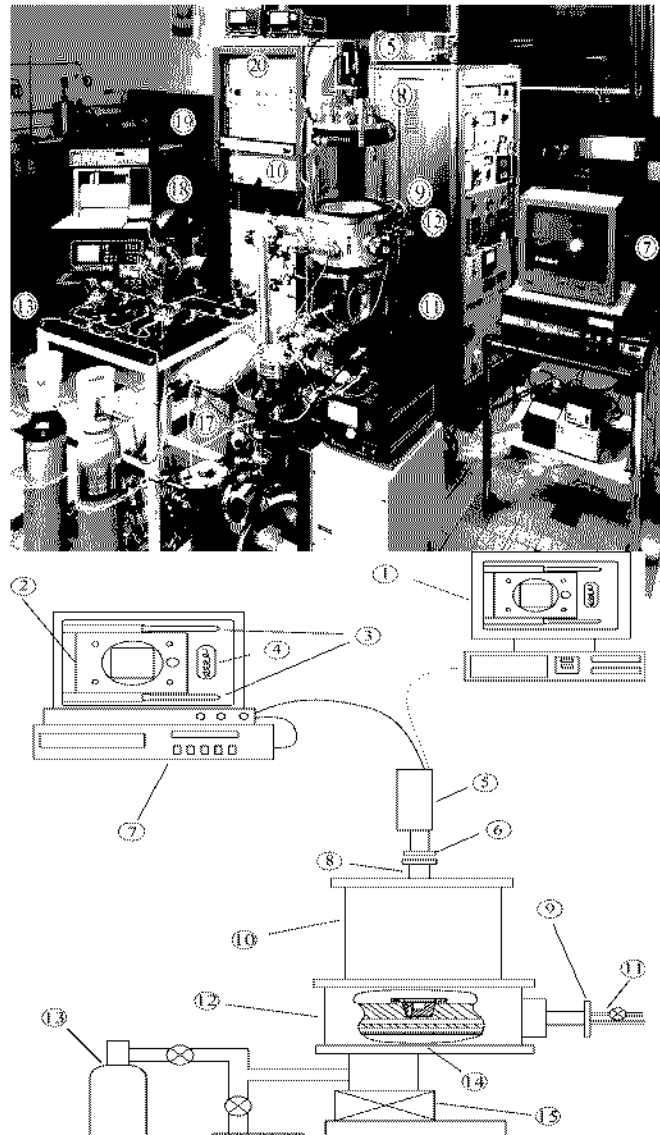
period in materials with high surface active species and underlines the importance of the thermocapillary flow, compared to other convection currents. In fact, low sulfur steels show relatively stable melt and solidification sections.

Table 1

	304LS	304HS	LS/HS	316LS	316HS	LS/HS
Front Surface (mm2)	31	31	100	78	82	95
Back Surface (mm2)	14	22,5	62,2	50	80	63
Front /Back Surface	44,6	72,5		64,5	97,5	

3.2 Cooling and Solidification

Depending on the residual chemistry of the investigated materials, mainly two types of liquid movements during the solidification stage have been observed. In case of very pure materials with temperature distribution of Figure 3 left, the liquid movement is not affected by solidification which remains invariably outwards. Similarly in case of materials with high level of surface active species, the movement in solidification phase remains inwards as during the melting stage. However in case of some materials with low levels of surface
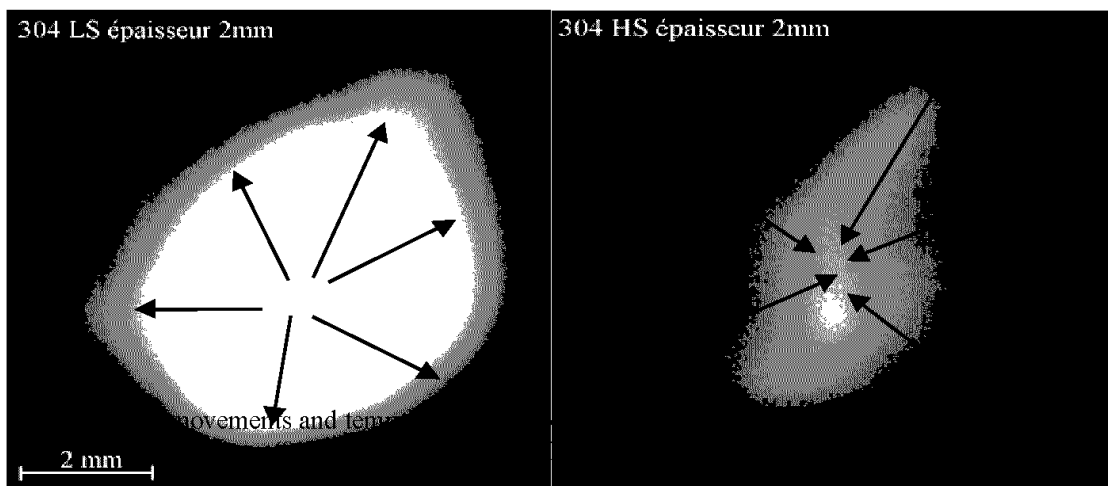
active elements, inversion in liquid movement has been seen during solidification in its early period. The liquid movement suddenly becomes inwards from the advancing solid liquid interface. In the first phase of solidification, liquid displacements occur at very high rate, reaching about 40mm/s and then slow down to 10mm/s, very close to the solidification rate as the interface progresses towards the center of the melt. This has been observed in case of a industrial Inconel 82 through particle displacements in the molten pool (Figure 5) and is interpreted as surface tension temperature inversion close to the solid-liquid interface i.e., dγ /dT changes from minus to plus due to solute redistribution. In fact, sulfur has a very low solubility in solid phase i.e., has low partition coefficient, and is rejected to the liquid by the advancing solid-liquid interface. A local concentration gradient is established just at the interface (Figure 6), sufficient to change local dγ/dT. Liquid movement in then reversed comparative to that in normal conditions, which is outwards in case of low sulfur materials. From theoretical standpoint, the inversion in liquid displacement would occur when the following condition is satisfied
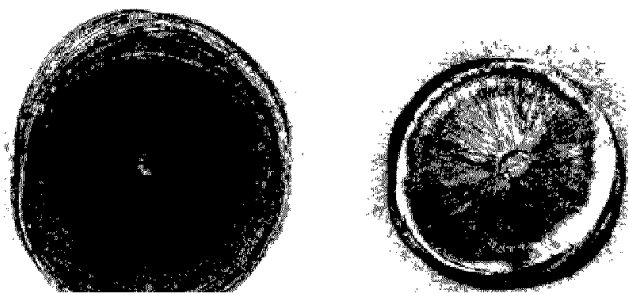
Fig.4 Back surface solidified sections, high – 80ppm sulphur (left), low-20ppm sulphur (right)
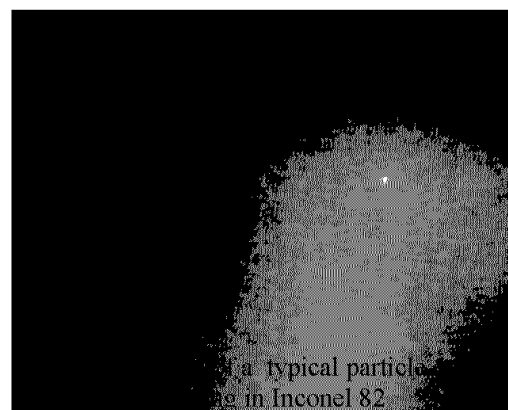
$$\frac{\partial \gamma}{\partial r} = \frac{\partial \gamma}{\partial T}\frac{\partial T}{\partial r} + \frac{\partial \gamma}{\partial C}\frac{\partial C}{\partial r} < 0$$
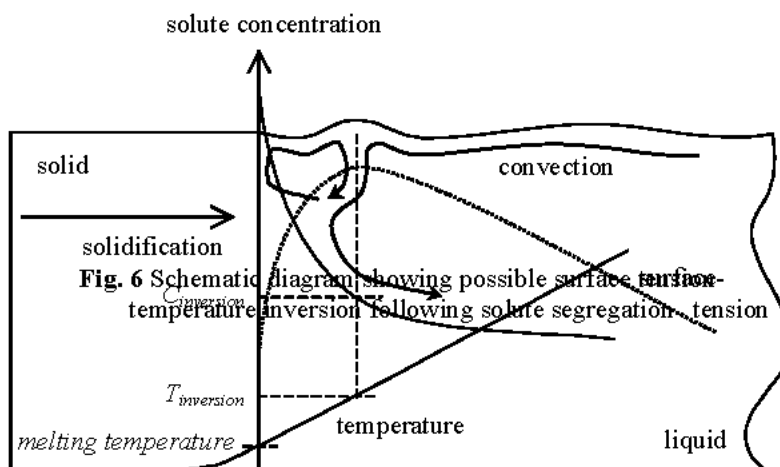
[1]

By hypothesis, on the basis of the observed outward convection currents in the molten pool, it may be assumed that at every point of the molten pool $\dfrac{\partial \gamma}{\partial T} < 0$ and in the solidification phase $\dfrac{\partial T}{\partial r} < 0$. Consequently, the first term of equation 1 is positive. Further, it is known that in case of materials where surface active species effectively operate , the surface tension concentration gradient is negative i.e., $\dfrac{\partial \gamma}{\partial C} < 0$. As in case of a non soluble solute , the concentration gradient $\dfrac{\partial C}{\partial r} > 0$, the second term in equation 1 becomes subsequently positive. Thus the mathematical condition for liquid inversion may be written as
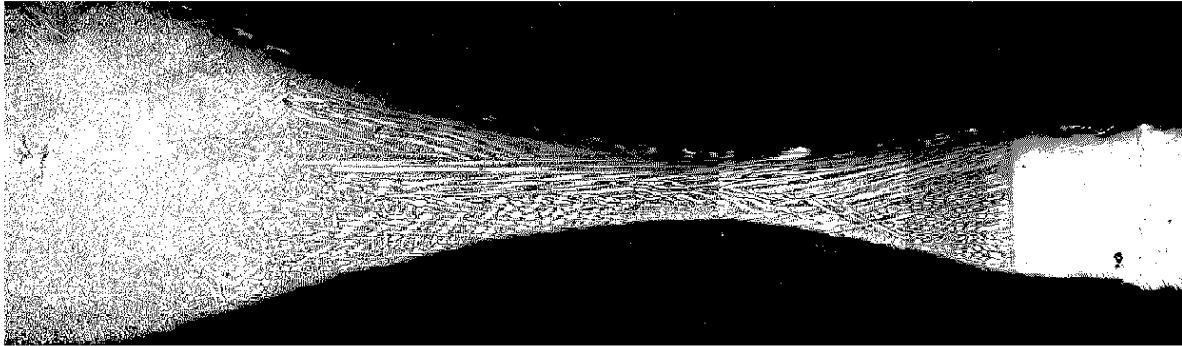
$$\left| \frac{\partial \gamma}{\partial T} \frac{\partial T}{\partial r} \right| < \left| \frac{\partial \gamma}{\partial C} \frac{\partial C}{\partial r} \right|$$

On this basis, whatever be the inversion motor, the mechanism of inversion can pursue with the solid-liquid interface as the motivating factor i.e., solute segregation pursues all along the solidification process as schematically shown in Figure 6.

The generated convection currents are sufficiently important enough to transport a significant amount of liquid towards the center of the molten pool. Thus specimen profiles in case of 0,5 mm thin specimens (Figures 7 & 8) can become as thick as 1 mm in the central part after solidification. Starting from the base non melted metal, the specimen as shown in Figure 7 becomes progressively thicker which implies that liquid displacement occurs in the direction of the center of the molten zone. Subsequently, the specimen becomes progressively thicker, though the material in the heating stage showed outward liquid displacement indicating a negative surface tension temperature gradient. This represents a very high liquid displacement induced by surface tension driven currents. The profile measurements of Figure 8 further show how liquid displacements are affected by material microchemistry. Whereas in inconel 82, swelling in the central region is observed, depression or thickness reduction is found on pure nickel in its central part. It may be recalled that, outward liquid displacement was observed during heating as well as during cooling stages. The difference in surface levels has been found to increase with the intensity of convection currents[5].


Fig. 6 Schematic diagram showing possible surface-temperature inversion following solute segregation

Fig.7 Thickening from the base metal (extreme right) to the centre(extreme left) after complete solidification on Inconel 82

**Pure Nickel**   **Inconel 82**
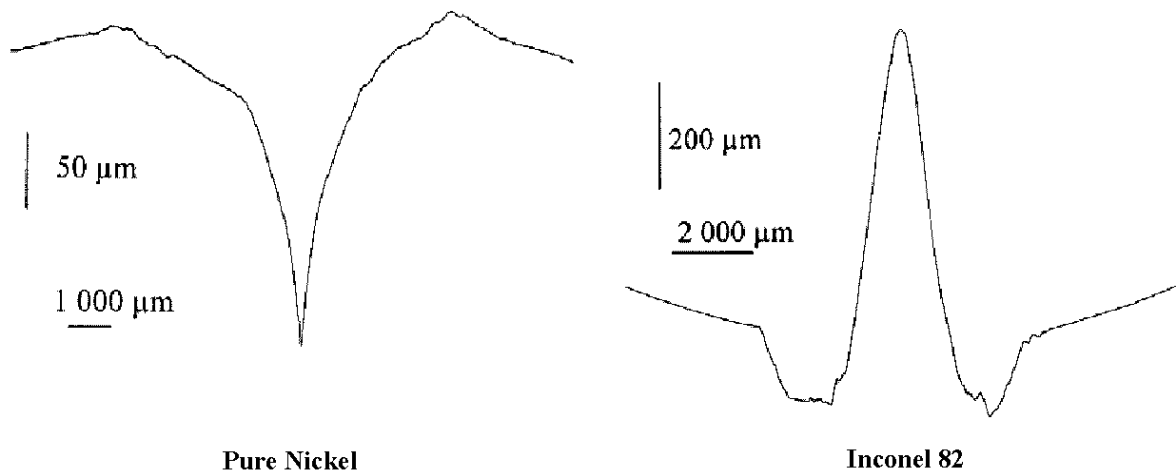
Fig.8 : Modification of surface profile according to the direction of liquid flow in the molten zone. Central depression in pure Nickel (outward flow) and swelling in Inconel (inward flow)

Figures 9 & 10 outline the difference resulting from liquid movements reported in 3.1 and observed after complete solidification. In case of pure nickel, where outward liquid displacements through floating particles was observed during the heating period, the cooling period resulted in clean central zone, which is last to solidify. The particles remain confined to the outer zone. The reverse is seen in case of high sulfur (80ppm) stainless steel where floating particles remained confined to the central zone both during the heating and the cooling period. It may be recalled that in this stainless steel material high depth to width ratio TIG welds and high back fusion sections were observed.
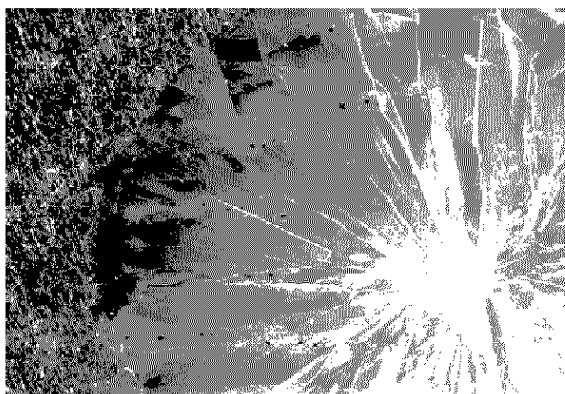
Fig.9 Particles in the outer solidification zone in pure Nickel
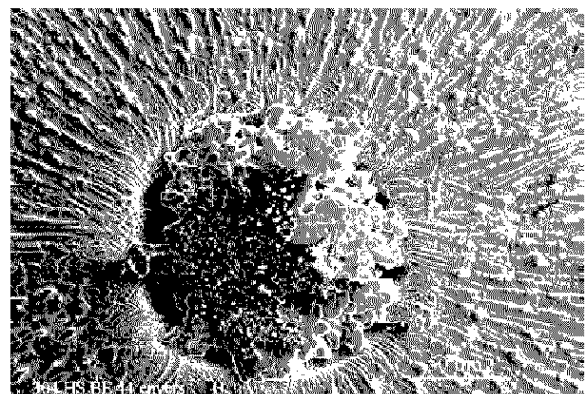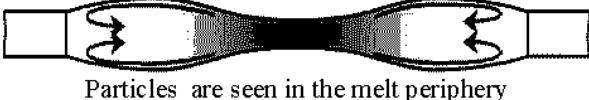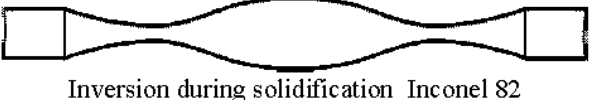

Fig.10 Particle concentration in the last solidified central zone, 80ppm stainless steel

203

4 Conclusions and perspectives

The results presented here are partially derived from the thesis work[5] and summarize the importance of convection currents as influenced by the microchemistry of the materials and temperature gradients in the molten pool. Further, it has been shown that even in materials with low concentration of surface active species, where outward liquid displacements in heating cycle are observed, surface tension temperature inversion may occur during the solidification period. This change is related to solute segregation particularly when solute partition coefficient is low and cooling is fast, as in the experiments presented here. Due to the very small specimen thickness, surface morphology after solidification is appreciably modified depending on the direction of convection currents.

Table 2

Supposed surface during heating	Real solidified surface profile
Particles are seen in the melt periphery	Normal convection . No or very low surface active species – Pure Nickel , Stainless steel-20ppm sulfur
Particles are seen in the melt periphery	Inversion during solidification Inconel 82
No outer particles, but strong central hot spot	Identical convection modes during melting & solidification, stainless steel- 80ppm sulfur

The table 2 summarizes the surface profiles observed during and after solidification. Further through particle displacement in the molten pool recorded by video, liquid movements as high as 40mm/s in the immediate phase of solidification have been measured. These speeds are much higher than the normal driven gravity flows. Though further investigations are still required, it seems that in materials with a high level of surface active species, grains are more refined. But this may be related to grain nucleation low purity materials. It would be interesting to compare two heats differentiating only in surface active species.

Acknowledgements

References

[1] C. R. Heiple and J. R. Roper: *Welding journal*, 61(1982), p 97s

[2] K. C. Mills and B. J. Keene: *International Materials Review*, 35(1990), p 185

[3] S. Kou and Y. H. Wang: *Welding journal*, 6((1986), p 63s

[4] M. Holt, D.L.Olson and C. E. Cross: *Scripta Metallurgica & Materialia*, 26(1992), p 1119

[5] L. Domergue: *Thèse de Doctorat*, ED 82-289, Ed ECN (1997)

[6] A. Shahab, S. Marya, and J. Binard: *Proc. Int. Conf on joining of Materials*, Helsingor (1990), p 395